



EVOLUTION OF TEXTURAL PARAMETER DURING THE FORMATION OF MCM-41 MESOPOROUS SILICA

Tewfik ALI-DAHMANE,^{a,b,c,*} Lamia BRAHMI,^{d,e} Naceur BENCHADRIA^{a,c} and Rachida HAMACHA^a

^aLaboratory of Materials Chemistry (LCM), University of Oran 1 Ahmed Ben Bella, BP 1524, El-Mnaouer, 31000 Oran, Algeria

^bLaboratory of Organic Electrolytes and Polyelectrolytes Application (LAEPO),
University Abou Beker Belkaid Tlemcen, BP119, 13000 Tlemcen, Algeria

^cHigher School of Applied Sciences of Tlemcen (ESSA-Tlemcen), P.O. Box 165, 13000 Bel Horizon, Tlemcen, Algeria

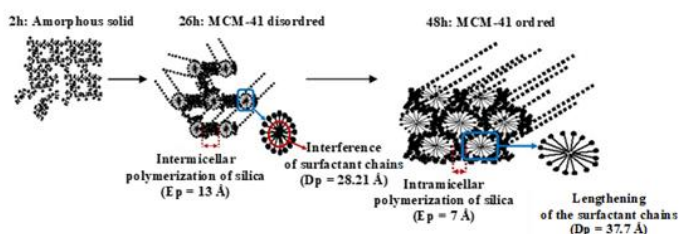
^dLaboratory of Fine Chemistry (LCF), University of Oran 1 Ahmed Ben Bella, P.O. Box 1524 El-Mnaouer, 31000 Oran, Algeria

^eDepartment of Chemistry, Faculty of Science, University Abou Beker Belkaid Tlemcen, BP 119, 13000 Tlemcen, Algeria

Received March 9, 2024

Mesoporous silica materials such as MCM-41 are widely studied for their ordered pore structures and high surface areas. Despite extensive research, the kinetic mechanisms governing their formation remain not fully understood. In this study, we investigate the time-dependent formation of Si-MCM-41 synthesized at 373 K using cetyltrimethylammonium bromide as a template, with colloidal silica as the silicon source. A series of samples was synthesized at different time intervals, and their structural and textural evolution was characterized using X-ray diffraction (XRD) and nitrogen adsorption measurements.

The results reveal a clear transition from an amorphous, non-porous phase to a highly ordered hexagonal mesostructure. The optimal material, obtained after 48 h of synthesis, exhibits a surface area of 1249 m²·g⁻¹ and a pore diameter of 37.7 Å. A three-stage mechanistic model is proposed, highlighting the competing effects of intermicellar and intramicellar silica polymerization during the synthesis. This kinetic study offers new insights into the mechanism of MCM-41 formation and provides a practical basis for optimizing synthesis conditions to tailor mesoporous silica properties.



INTRODUCTION

The mesoporous molecular sieve MCM-41 is a well-known member of the M41S family of mesoporous materials, first discovered by the Mobil Research group in the early 1990s.^{1,2} These materials are synthesized through hydrothermal treatment of silica gel or aluminosilicate precursors in the presence of a structure-directing agent.

Although the crystallization mechanism differs from that of zeolites, the synthesis method is similar in terms of temperature and processing conditions. MCM-41 materials possess uniform mesopores with tunable diameters ranging from 20 to 100 Å, high surface areas, and excellent thermal stability. These features make them highly attractive for various applications, particularly in catalysis^{3–8} and adsorption.^{9–12}

* Corresponding author: byalidahmane@gmail.com

The synthesis of MCM-41 typically proceeds via one of three templating pathways: the ionic S^+I^- mechanism, where cationic surfactants (*e.g.*, CTAB) interact with anionic silicate oligomers; the $S^+X^-I^+$ route, involving ion pairs formed with halide anions ($X^- = Cl^-, Br^-$) and cationic inorganic species (I^+); and the neutral S^0I^0 route. Upon assembly, template removal, usually via calcination, is necessary to generate the final porous structure. For materials synthesized via the S^+I^- or $S^+X^-I^+$ pathways, calcination or solvent extraction followed by calcination is commonly employed.

Over the past three decades, many researchers have explored the mechanism of MCM-41 formation. The original Mobil work proposed a liquid-crystal templating (LCT) route.² Chen *et al.*¹³ suggested that ordered mesostructures could also arise from isotropic surfactant-silicate solutions, supporting a cooperative self-assembly process. Galarneau *et al.*,¹⁴ using in situ EPR measurements with spin-probe molecules, investigated MCM-41 formation at 323 K and observed a transition from a disordered hybrid phase to an ordered hexagonal structure. More recently, Candela-Noguera *et al.*¹⁵ examined the effects of stirring intensity and surfactant addition rate on the mesostructure formation, providing additional insight into synthesis parameters.

Despite these efforts, relatively few studies have investigated the kinetic evolution of purely siliceous MCM-41 using time-resolved textural and structural characterization. Blin *et al.*¹⁶ conducted a kinetic study using sodium silicate and CTAB as precursors, showing that pore diameter remained constant while wall thickness increased significantly with synthesis time and temperature.

To optimize MCM-41 for adsorption and catalytic performance, a detailed understanding of how structural features, such as wall thickness and pore architecture, evolve during synthesis is essential. However, the interplay between synthesis time, silica polymerization, and surfactant interactions remains insufficiently understood.

In this work, we investigate the kinetic formation of Si-MCM-41 synthesized at 373 K using cetyltrimethylammonium bromide (CTAB) as a structure-directing agent, and colloidal silica as the silicon source. A series of samples was synthesized at different time intervals, and their textural and structural evolution was evaluated by X-ray diffraction (XRD) and nitrogen adsorption analyses. Our results reveal a three-stage formation process, which we compare to previously proposed models (Galarneau and Blin) to refine the understanding of

mesoporous silica self-assembly. The findings offer new insights into the time-dependent development of MCM-41 and provide practical guidelines for synthesis optimization.

EXPERIMENTAL

Preparation of MCM-41 samples

All chemicals were used as received without further purification. Cetyltrimethylammonium bromide (CTAB, 99%) was purchased from Acros. Tetramethylammonium hydroxide (TMAOH, 5H₂O, 97%) and colloidal silica (LUDOX HS-40, 40 wt.% SiO₂) were obtained from Prolabo. Deionized water was used in all syntheses.

Si-MCM-41 was synthesized using a hydrothermal method. The molar composition of the synthesis gel was: SiO₂ : 0.25 CTAB : 0.20 TMAOH : 40 H₂O. The selection of molar ratios was based on the work of Mokaya *et al.*,¹⁷ who highlighted the importance of precise surfactant-to-silica ratios in achieving well-ordered MCM-41 structures with uniform mesopore sizes and high specific surface areas. In the present study, the CTAB/Si ratio was carefully optimized to stabilize micellar assemblies and to enhance both the rate and uniformity of silica condensation under mildly basic conditions, thereby promoting the formation of a highly ordered hexagonal mesostructure.

The synthesis of Si-MCM-41 was carried out in three main steps:

Formation of the hydrogel: 2.06 g of TMAOH was dissolved in 69.14 g of deionized water under stirring for 5 minutes. Then, 10.00 g of CTAB was slowly added to the solution while stirring was continued for an additional 25 minutes. Subsequently, 16.46 g of colloidal silica was added dropwise under vigorous stirring, and the mixture was stirred for a further 1 hour to ensure homogenization.

Hydrothermal treatment: the hydrogel obtained in the first step was transferred into a Teflon-lined autoclave and subjected to hydrothermal crystallization at 373 K for various durations: 2 h, 6 h, 20 h, 26 h, 30 h, 48 h, 72 h, and 120 h. The crystallization process was halted by cooling the autoclave under running water. The resulting solid was then recovered by filtration, thoroughly washed with deionized water, and dried at 373 K overnight.

Calcination: After the hydrothermal treatment, the solid product was calcined in a muffle furnace under static air at 823 K for 12 hours, using a heating rate of 2 K/min, in order to remove the

organic surfactant and reveal the mesoporous framework. This calcination step was essential to ensure the formation of a well-ordered porous structure characteristic of MCM-41.

Characterization of MCM-41 samples

The structural characterization was carried out by powder X-ray diffraction (XRD) using a PHILIPS PW 3710 diffractometer with $\text{CuK}\alpha$ (wavelength (λ) = 1.5406 Å) radiation, operated at 40 kV and 40 mA. Measurements were performed over the 2 theta range of 2° to 10°, with a step size of 0.02° and a counting time of 1 second per step. An apparatus of the type Micromeritics GEMINI 2375 type was used for the textural characterization by using the adsorption of nitrogen at 77 K. Before the measurements, and samples were degassed under vacuum for at least 24 hours at 473 K.

The properties of the measured samples were determined as follows:

The interplanar spacing (d_{100}) was calculated by the equation $\lambda = 2d_{100} \sin\theta$. The unit cell parameter (a_0) of the hexagonal mesoporous structure was estimated using the relation $a_0 = 2/(3)^{1/2} \cdot d_{100}$. The pore diameter (D_p) was calculated according to the following expression:

$$D_p = c \cdot d_{100} [\rho \cdot V_{\text{meso}} / (1 + \rho \cdot V_{\text{meso}})]^{1/2},$$

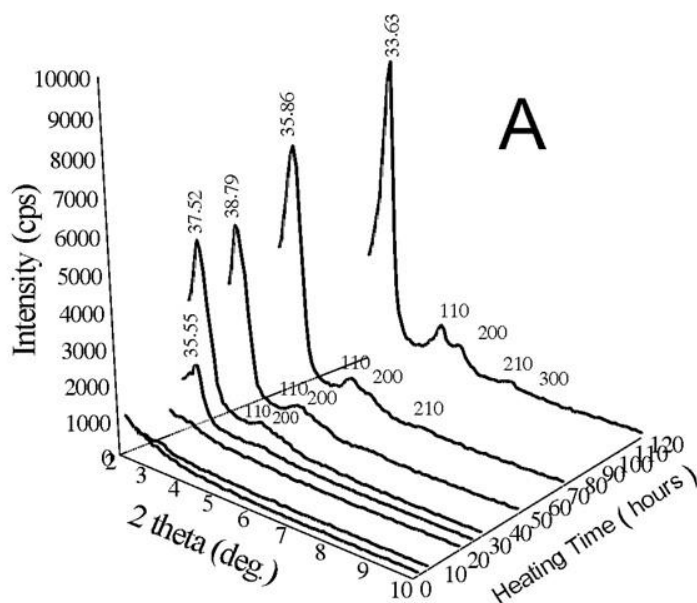
where V_{meso} is mesoporous volume obtained by using the t-plot method, ρ is the density of the walls pores ($2.2 \text{ cm}^3 \cdot \text{g}^{-1}$ for silica materials),¹⁸ d_{100} is

interplanar spacing, and c is a constant depending on the pore geometry ($c = 1.213$ for a geometry cylindrical²). The wall thickness (E_p) was calculated as the difference between the unit cell parameter and the pore diameter: $E_p = a_0 - D_p$. The specific surface area (S_{BET}) was determined using the Brunauer-Emmett-Teller method.¹⁹

RESULTS AND DISCUSSION

X-ray diffraction

The X-ray diffractogram (XRD) of the MCM-41 is characterized by an ordered structure consisting of four peaks of Bragg to weak angles of diffraction between 2 and 7° (2 theta), which can be indexed with a hexagonal network: (100), (110) and (200)^{20,21}. The XRD indicates that the obtained phases are not crystalline, as no diffraction peaks are observed at high angles. According to Cheng *et al.*,²² the use of the term “*crystalline*” is appropriate only when the material exhibits a well-preserved periodic arrangement of channels, which represents the essential element of structural order in MCM-41. Figure 1 represents the kinetic evolution by XRD of the Si-MCM-41 samples synthesized at different heating time. Each diffractogram is indexed by the corresponding interplanar spacing (d_{100}).



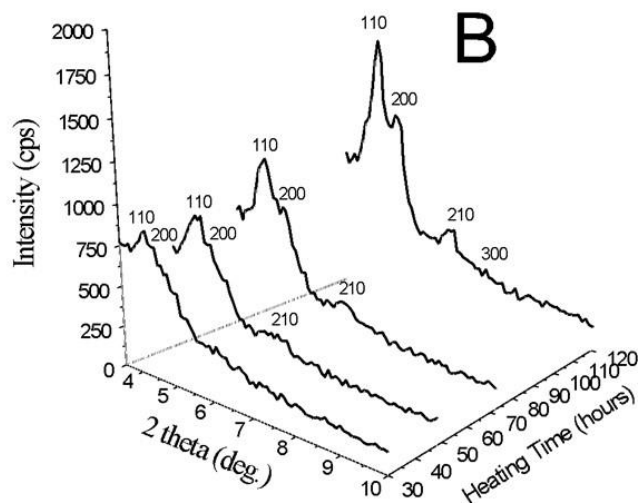


Fig. 1 – XRD patterns of Si-MCM-41 samples synthesized at different heating times: **A**) Wide-angle range (2θ : $2\text{--}10^\circ$) showing the evolution of all diffraction peaks including the (100) reflection; **B**) Zoomed-in view (2θ : $4\text{--}10^\circ$) focusing on the development of higher-order reflections (110), (200), (210), and (300).

Between 2 and 20 hours of synthesis, amorphous products are obtained (absence of the diffraction peak (100)). The beginning formation of the Si-MCM-41 formation take place after 26 hours of reaction. For this synthesis time, we observe the absence of peaks the (110), (200), and (210) peaks, which suggests a disordered structure of Si-MCM-41. Beyond that time, the intensity of the (100) peak and the interplanar spacing (d_{100}) increase with the synthesis time. In the same way, the peaks corresponding to the other reflections (110), (200), and (210) appear and apparent, revealing a better ordered hexagonal structure of the mesoporous channels in MCM-41.² The appearance of the (300)

peak after 5 days of synthesis demonstrates that the material not only maintains its stability following calcination at 823 K for 12 hours but also achieves an enhanced degree of structural order.

N_2 -sorption

Si-MCM-41 is characterized by an isotherm of type IV according to the BDDT classification.²³ This isotherm is defined by three stages: the monolayer-multilayer adsorption of N_2 on the walls of the mesopores, the capillary condensation of nitrogen within the mesopores and then multilayer adsorption on the external surface of the particles.

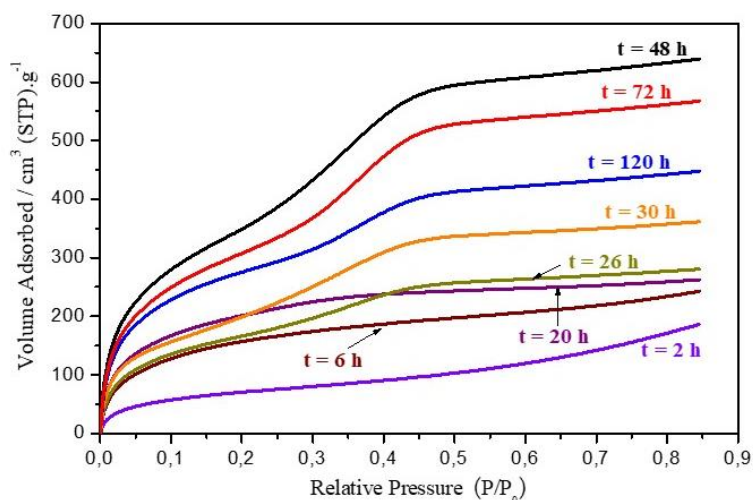


Fig. 2 – N_2 -Adsorption isotherms of Si-MCM-41 samples synthesized at different heating times.

For a synthesis time of 2 hours, a type II isotherm is obtained, which characterizes amorphous nonporous solids (Fig. 2). From 6 hours until 20 hours, the isotherms become types I+IV (super-microporous solid of diameters between 15 and 20 Å)²⁴ and the capillary condensation stage is not clearly observed. This is due to the presence of an important quantity of amorphous phase in the sample.¹⁶ The type IV isotherm characteristic of mesoporous solids is observed after 26 hours of synthesis. Beyond this time, the same isotherm type is maintained, but the adsorbed quantity decreases when the synthesis time exceeds 48 hours.

Pore diameter

When the template with various lengths of alkyl chains is used for the synthesis of the MCM-41, the samples obtained will have various pore diameters.^{1,2} Figure 3 shows that the pore diameter depends strongly on the heating time. For longer durations, a more extended surfactant molecular conformation can be obtained, which leads to materials with larger pore sizes. The pore diameter that characterizes the Si-MCM-41 is obtained after 48 h of synthesis.

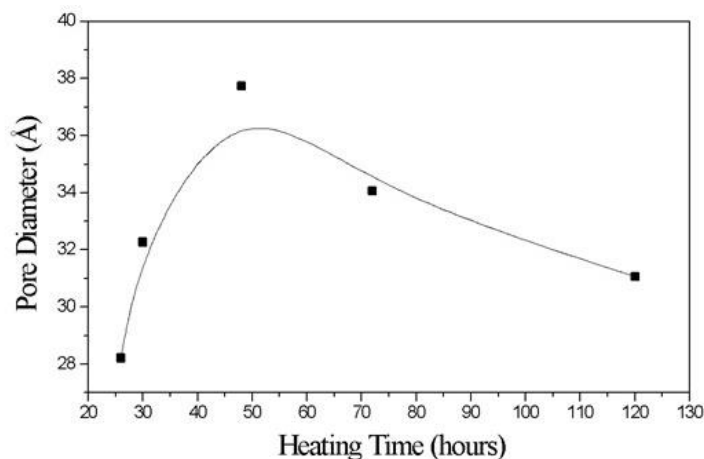


Fig. 3 – Evolution of the pore diameter (D_p) of Si-MCM-41 samples synthesized at different heating times.

Mesoporous volume and the wall thickness

The beginning of the formation of the Si-MCM-41 is characterized by a significant wall thickness (13 Å). Beyond this time (26 hours), the reduction is clearly observed and it is minimal after 48 h of reaction (7 Å) (Fig. 4). The same evolution as for

the wall thickness is observed for S_{BET} (Table 1) and V_{meso} . Once Si-MCM-41 is formed (26 hours), we observe an increase in S_{BET} and V_{meso} until obtaining an optimum of 1249 $m^2 \cdot g^{-1}$ and 0.82 $cm^3 \cdot g^{-1}$, respectively, for 48 hours of synthesis. These values characterize the purely siliceous mesoporous MCM-41 material.²⁵

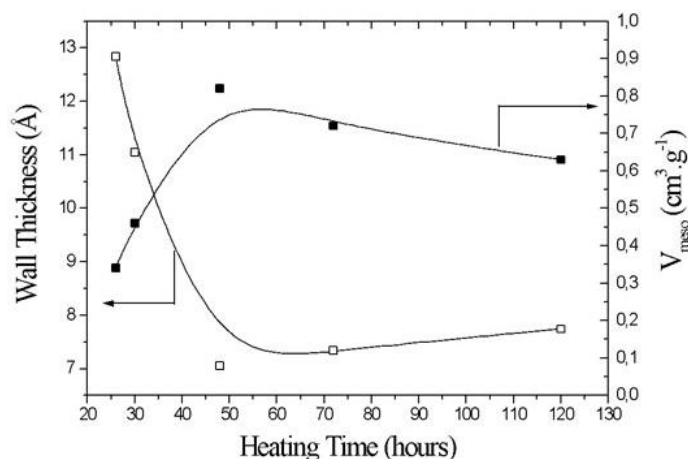


Fig. 4 – Evolution of the walls thickness (E_p) and the mesoporous volume (V_{meso}) of Si-MCM-41 samples synthesized at different heating times.

Table 1
 S_{BET} for Si-MCM-41 samples synthesized at different heating times

Heating time (h)	2	6	20	26	30	48	72	120
S_{BET} ($\text{m}^2 \cdot \text{g}^{-1}$)	255	567	591	712	942	1249	1189	1106

The most ordered structure with the highest S_{BET} , is obtained for 48 hours of synthesis. The values of the wall thickness and the pore diameter obtained for this synthesis time correspond to a stable mesoporous Si-MCM-41 material suitable for use as a catalyst or adsorbent.

Mechanistic explanation

In synthesizing mesoporous materials, a mineral layer is interposed between micelles of a lyotropic phase (liquid crystals). A mechanism proposed under various models suggests that the interaction between silicates and the template acts as a force that leads to the formation of structures that determine the final nature of mesoporous materials. Among these models, the model of Beck *et al.* (1992)² consists of three stages: (i) formation of spherical micelles, (ii) arrangement of micelles in hexagonal form (iii) polymerization of silica on hexagonal micelles.

In the model proposed by Chen *et al.*,¹³ the micelles are in a disordered rod-like form and interact with silicate species to form multiple silica monolayers on the external surface of the micelles, followed by spontaneous assembly to produce the hexagonal structure.

A study carried out by Galarneau *et al.*,¹⁴ based on in situ EPR measurements with spin-probe molecules, demonstrated the various structural and dynamic changes occurring in the organic/inorganic hybrid systems. Two stages are highlighted by coupling these two techniques: an ionic exchange of counter-ions of quaternary ammoniums by ions silicates and a lengthening slowly of cylindrical micelles while organizing itself to form an ordered hexagonal phase after the disappearance of a disordered phase. The final stage is controlled by the condensation kinetics of the silicate species, which coat the cylindrical micelles and form the material's wall thickness.

Blin *et al.*¹⁶ optimized the synthesis conditions using cetyltrimethylammonium bromide and sodium silicate as the template and silica sources, respectively. Based on the characterization results, the synthesis mechanism was postulated as follows: (i) hydrolysis and condensation of the silica source, (ii) polycondensation of the silica source around the

cylindrical micelles, and (iii) an increase in the wall thickness while the pore size remains constant.

Considering this information about the mechanism of Si-MCM-41 and the proprieties obtained in this work, we have tried to make a relation between the textural properties and the mechanism of formation:

Between 6 and 26 hours of synthesis, we have the structure evolution from amorphous solids (XRD) to types I+IV isotherms characteristic of the super-microporous solids whose S_{BET} is between 567–591 $\text{m}^2 \cdot \text{g}^{-1}$.

For a time of 26 hours, we obtained the peak corresponding to characteristic reflection (100) of Si-MCM-41 with considerable properties ($D_p = 28.21 \text{ \AA}$, $E_p = 12.84 \text{ \AA}$, $S_{\text{BET}} = 712 \text{ m}^2 \cdot \text{g}^{-1}$ and $V_{\text{meso}} = 0.3 \text{ cm}^3 \cdot \text{g}^{-1}$). By XRD and N_2 -adsorption analysis, the sample obtained after 48 h of synthesis has shown 100% of crystallinity (better organization of the channels). We note that the wall thickness decreases by 45% to have a minimal value at 7 \AA , in this case, the S_{BET} and V_{meso} increase by 43% and 58.4% for maximum values of the order 1249 $\text{m}^2 \cdot \text{g}^{-1}$ and 0.82 $\text{cm}^3 \cdot \text{g}^{-1}$ respectively. The increase in V_{meso} and S_{BET} are correlated very well with the reduction of the wall thickness.

While based on Galarneau and Blin models and by using the system $\text{SiO}_2:0.25\text{CTABr}:0.2\text{TMAOH}:40\text{H}_2\text{O}$ at 373 K, our results give some details on the mechanism of formation of the mesoporous materials (Fig. 5):

[I] At the beginning of synthesis, between 2 and 20 hours, we obtained amorphous products due to the polymerization of silica (XRD: absence of the diffraction peak (100) and N_2 -sorption: the capillary condensation of nitrogen within the mesopores is not observed).

[II] At 26 hours, the MCM-41 is obtained with weak organization of the channels (XRD: absence of peaks (110) and (200) and N_2 -sorption: the capillary condensation of nitrogen within the mesopores is observed, but the volume of nitrogen adsorbed is low) due to the prevalence of intermicellar polymerization of the silica ions ($E_p = 13 \text{ \AA}$), compared with the ionic exchange between the counter-ions of template and the silicate ions without significant lengthening of the channels ($S_{\text{BET}} = 712 \text{ m}^2 \cdot \text{g}^{-1}$ and $V_{\text{meso}} = 0.3 \text{ cm}^3 \cdot \text{g}^{-1}$) and interference of surfactant chains ($D_p = 28.21 \text{ \AA}$).

[III] When the heating time increases until 48 hours, the Si-MCM-41 is obtained with a better organization of the channels (XRD: the peaks (110) and (200) appear and N_2 -sorption: the capillary condensation step is quite evident, and the volume of nitrogen adsorbed is the highest) due to the prevalence of the ionic exchange between counter-ions of template and silicate ions ($E_p = 7 \text{ \AA}$) compared to the intermicellar polymerization of the silica ions ($S_{BET} = 1249 \text{ m}^2 \cdot \text{g}^{-1}$ and $V_{\text{meso}} = 0.82 \text{ cm}^3 \cdot \text{g}^{-1}$) and the lengthening of the surfactant chains ($D_p = 37.7 \text{ \AA}$).

Beyond 48 hours a slight reduction in S_{BET} and V_{meso} is observed, likely due to the depolymerization of silica, which condenses on the walls of the channels. This condensation results in an increase in wall thickness. It can also be hypothesized that, after a certain duration, the template is completely depleted, and the excess silica further thickens the channel walls. Under these conditions, there is a prevalence of intermicellar polymerization of silica, which dominates the mechanism at this stage.

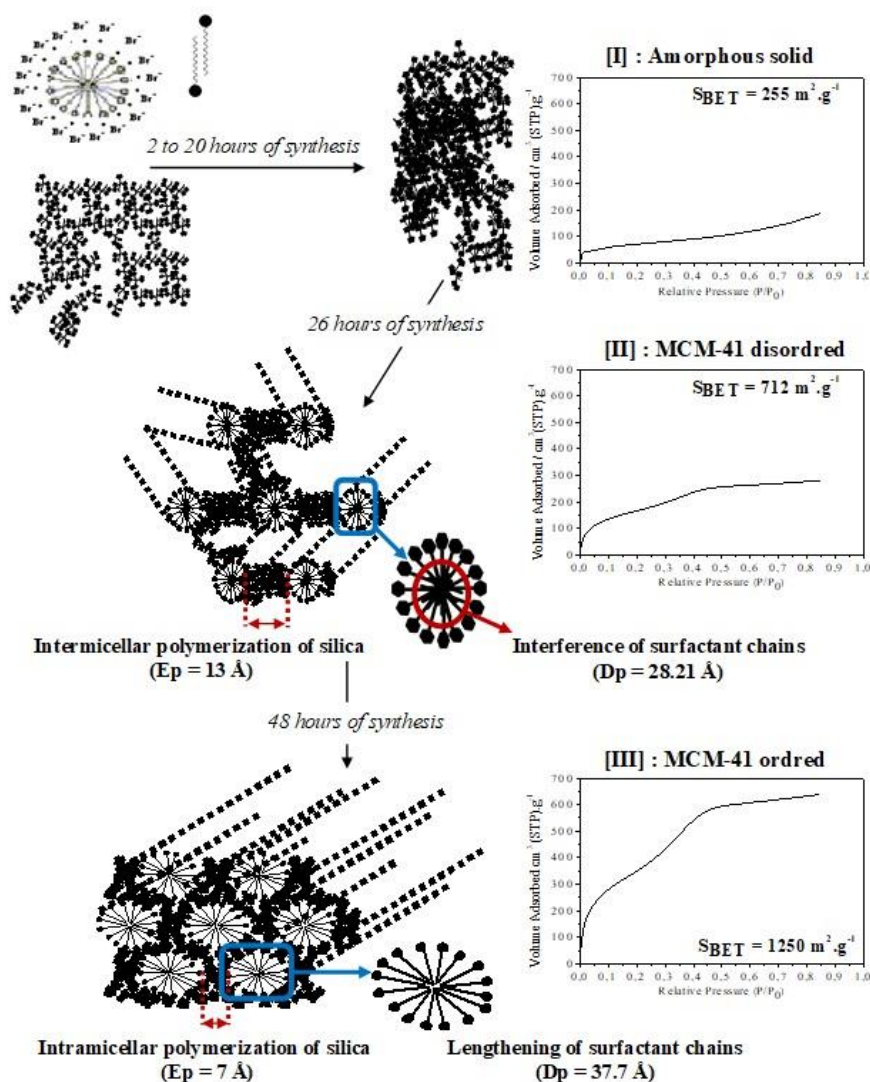


Fig. 5 – Schematic representation of the proposed mechanism of MCM-41 formation: [I] Formation of the amorphous product by silica polymerization. [II] Formation of MCM-41 disordered due to the prevalence intramicellar polymerization of silica. [III] Arrangement of the channels and formation of ordered MCM-41 driven by the prevalence of intermicellar polymerization of silica.

CONCLUSIONS

The kinetic study of Si-MCM-41 formation at 373 K revealed a clear time-dependent evolution in both porosity and structural organization. The

material was initially amorphous and nonporous, then evolved into a supermicroporous phase, and ultimately developed into a well-ordered mesoporous structure. A highly organized MCM-41 framework emerged after 26 hours of synthesis,

with the optimal textural properties, including maximum surface area, mesopore volume, and minimum wall thickness, achieved around 48 hours. Beyond this period, a gradual decline in mesostructural order and textural performance was observed. These findings define an optimal synthesis period and provide valuable insights into the structural and textural evolution of mesoporous silica over time.

In addition to identifying the optimal synthesis conditions, this study proposes a refined three-stage mechanistic model for the formation of MCM-41. Developed through critical comparison with the models of Galarneau and Blin, the proposed approach deepens the current understanding of the cooperative self-assembly between silicate species and surfactant micelles. It offers a more comprehensive mechanistic interpretation of mesostructure development and constitutes a significant contribution to the field of mesoporous materials chemistry.

REFERENCES

1. T. Yanagisawa, T. Shimizu, K. Kudora and C. Kato, *Bull. Chem. Soc. Jpn.*, **1990**, *63*, 988–992.
2. J. S. Beck, J. C. Vartuli, W. J. Roth, M. E. Leonowicz, C. T. Kresge, K. D. Schmitt, C. T. W. Chu, D. H. Olson, E. W. Sheppard, S. B. McCullen, J. B. Higgins and J. L. Schlenker, *J. Am. Chem. Soc.*, **1992**, *114*, 10834–10843.
3. L. Brahmi, T. Ali-Dahmane, R. Hamacha and S. Hacini, *J Mol Catal A Chem*, **2016**, *423*, 31–40.
4. Y. Doussaid, T. Ali-Dahmane, N. Mehiaoui, L. Brahmi, Z. Kibou, R. Hamacha and N. Choukchou-Braham, *Lett. Org. Chem.*, **2021**, *18*, 1–6.
5. M. Ghadermazi and S. Molaei, *Inorg. Chem. Commun.*, **2023**, *147*, 110225.
6. L. L. Silva, I. W. Zapelini and D. Cardoso, *Silicon*, **2024**, *16*, 765–773.
7. M. Nikoorazm, B. Tahmasbi, S. Gholami, M. Khanmoradi, Y. Abbasi Tyula, M. Darabi and M. Koolivand, *Polyhedron*. **2023**, *244*, 116587.
8. Z. S. Robatjazi, M. R. Naimi-Jamal and M. Tajbakhsh, *Sci. Rep.*, **2022**, *12*, 4949.
9. A. Corma, A. Martínez, V. Martínez-Soria and J. B. Montón, *J. Catal.*, **1995**, *153*, 25–31.
10. A. Sayari, *Chem. Mater.*, **1996**, *8*, 1840–1852.
11. M. R. Oliveira, J. A. Cecilia, J. F. De Conto, S. M. Egues and E. Rodríguez-Castellón, *Sol-Gel Sci Technol.*, **2023**, *105*, 370–387.
12. D. M. Oliveira and A. S. Andrada, *Cerâmica*, **2019**, *65*, 170–179.
13. C. Y. Chen, S. L. Burkett, H. X. Li and M. E. Davis, *Microporous Materials*, **1993**, *2*, 27–34.
14. A. Galarneau, F. Di Renzo, F. Fajula, L. Mollo, B. Fubini and M. F. Ottaviana, *J. Colloid Interface Sci.*, 1998, *201*, 105–117.
15. V. Candela-Noguera, M. Alfonso, P. Amorós, E. Aznar, M. D. María Dolores Marcos, R. Ramón Martínez-Mañez, *Microporous Mesoporous Mater.*, **2024**, *363*, 112840.
16. J. L. Blin, C. Otjacques, G. Herrier and B. L. Su, *Int. J. Inorg. Mater.*, **2001**, *3*, 75–86.
17. R. Mokaya, *Microporous Mesoporous Mater.*, **2001**, *44-45*, 119–127.
18. M. Kruk, M. Jaroniec and A. Sayari, *J. Phys. Chem. B*. **1997**, *101*, 583–589.
19. S. Brunauer, P.H. Emmett and E. Teller, *J. Am. Chem. Soc.*, **1938**, *60*, 309–319.
20. T. Ali-Dahmane, L. Brahmi, R. Hamacha and A. Bengueddach, *Ann. Chim. Sci. Mat.*, **2017**, *40*, 149–163.
21. T. Ali-Dahmane, L. Brahmi, R. Hamacha, S. Hacini and A. Bengueddach, *Bull. Chem. React. Eng.*, **2019**, *14*, 358–368.
22. F. Cheng, W. Zhaou, D. H. Park, J. Klinowski, M. Hargreaves and L. F. Gladden, *J. Chem. Soc., Faraday Trans.*, **1997**, *93*, 359–363.
23. S. Brunauer, L. S. Deming, W. S. Deming and E. Teller, *J. Am. Chem. Soc.*, **1940**, *62*, 1723–1732.
24. E. Bastardo-Gonzalez, R. Mokaya and W. Jones, *Chem. Commun.*, **2001**, *11*, 1016–1017.
25. P. Selvam, S. K. Bhatia and C. G. Sonwane, *Ind. Eng. Chem. Res.*, **2001**, *40*, 3237–3261.